Bod1, a novel kinetochore protein required for chromosome biorientation

Iain M. Porter,[1] Sarah E. McClelland,[3] Guennadi A. Khoudoli,[1] Christopher J. Hunter,[2] Jens S. Andersen,[4] Andrew D. McAinsh,[3] J. Julian Blow,[1] and Jason R. Swedlow[1]

[1]Division of Gene Regulation and Expression and [2]Medical Research Council Protein Phosphorylation Unit, College of Life Sciences, University of Dundee, Dundee DD1 5EH, Scotland, UK
[3]Chromosome Segregation Laboratory, Marie Curie Research Institute, Oxted, Surrey RH8 0TL, England, UK
[4]Center for Experimental Bioinformatics, University of Southern Denmark, DS-5230 Odense, Denmark

We have combined the proteomic analysis of *Xenopus laevis* in vitro–assembled chromosomes with RNA interference and live cell imaging in HeLa cells to identify novel factors required for proper chromosome segregation. The first of these is Bod1, a protein conserved throughout metazoans that associates with a large macromolecular complex and localizes with kinetochores and spindle poles during mitosis. Small interfering RNA depletion of Bod1 in HeLa cells produces elongated mitotic spindles with severe biorientation defects. Bod1-depleted cells form syntelic attachments that can oscillate and generate enough force to separate sister kinetochores, suggesting that microtubule–kinetochore interactions were intact. Releasing Bod1-depleted cells from a monastrol block increases the frequency of syntelic attachments and the number of cells displaying biorientation defects. Bod1 depletion does not affect the activity or localization of Aurora B but does cause mislocalization of the microtubule depolymerase mitotic centromere-associated kinesin and prevents its efficient phosphorylation by Aurora B. Therefore, Bod1 is a novel kinetochore protein that is required for the detection or resolution of syntelic attachments in mitotic spindles.

Introduction

Mitotic chromosome segregation requires the coordination of both regulatory and mechanical molecular machines and culminates in the delivery of two complete sets of chromosomes to two daughter cells. Chromosomes contain long, continuous strands of DNA that are folded and assembled into higher order structures, which, in human cells, results in a 10–20,000-fold linear compaction of DNA (Swedlow and Hirano, 2003). Besides the core histones, many nonhistone chromosomal proteins have been identified (Uchiyama et al., 2005), but a full identification and functional characterization of chromosomal proteins has so far been unavailable.

Chromosomes assemble specific structures called kinetochores that serve as the molecular machines to mediate attachment, checkpoint signaling, and force generation at the ends of spindle microtubules (Cleveland et al., 2003; Tanaka et al., 2005). Kinetochores are built either at the primary constriction of centric chromosomes or along the whole length of holocentric chromosomes. The molecular components of kinetochores are best characterized in *Saccharomyces cerevisiae*, and many of the components of yeast kinetochores are highly conserved (De Wulf et al., 2003; Westermann et al., 2003; Cheeseman et al., 2004; Meraldi et al., 2006). Nonetheless, a full inventory of the components of the animal cell kinetochore is still lacking.

Cell-free cytoplasmic extracts from *Xenopus laevis* eggs have previously been used for functional studies of chromosomes and kinetochores (Hirano and Mitchison, 1994; Desai et al., 1997; Funabiki and Murray, 2000; Emanuele et al., 2005). This system targets many chromosome and kinetochore proteins to chromatin in a cell cycle–dependent fashion and has the advantage of providing a method of preparing chromatin and chromosomes that are largely free of cytoplasmic contaminants. We have previously developed methods for preparing a soluble fraction of chromatin and chromosome-associated proteins (Murnion et al., 2001) and have used two-dimensional gel electrophoresis of these preparations to reveal >350 distinct polypeptides associated with in vitro–assembled mitotic chromosomes, although the exact number depended on the resolution of the gel system (Khoudoli et al., 2004).

Correspondence to Jason R. Swedlow: jason@lifesci.dundee.ac.uk

Abbreviations used in this paper: ACA, anticentromere antibody; CENP, centromere protein; MCAK, mitotic centromere-associated kinesin; shRNA, short hairpin RNA.

The online version of this article contains supplemental material.

The Journal of Cell Biology, Vol. 179, No. 2, October 22, 2007 187–197
http://www.jcb.org/cgi/doi/10.1083/jcb.200704098

Supplemental Material can be found at:
http://www.jcb.org/cgi/content/full/jcb.200704098/DC1

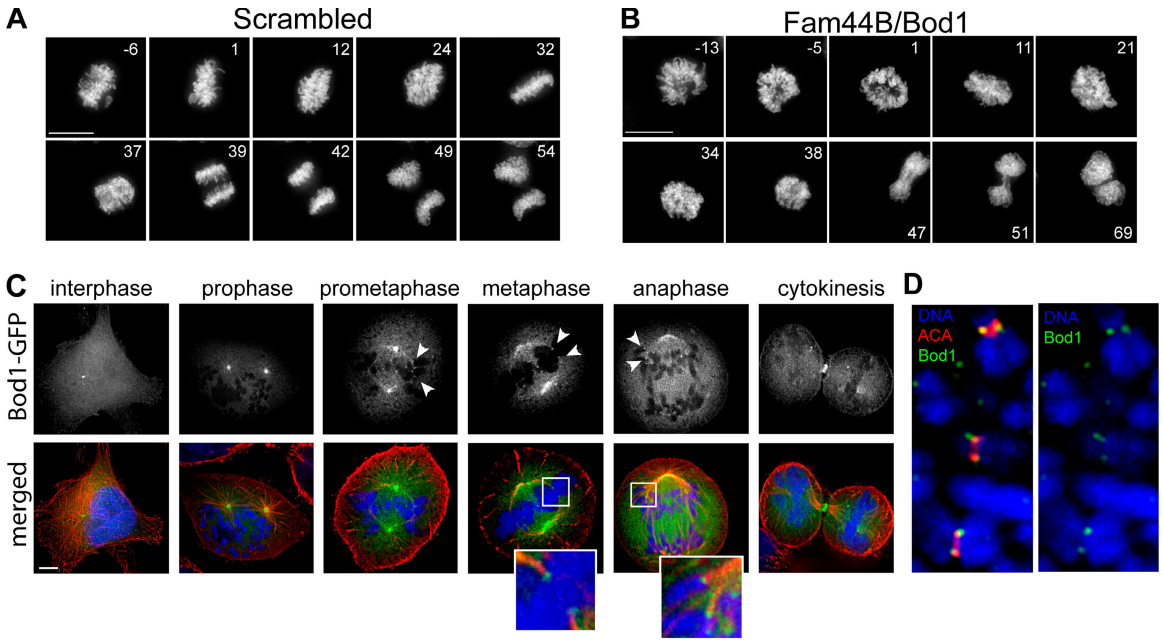

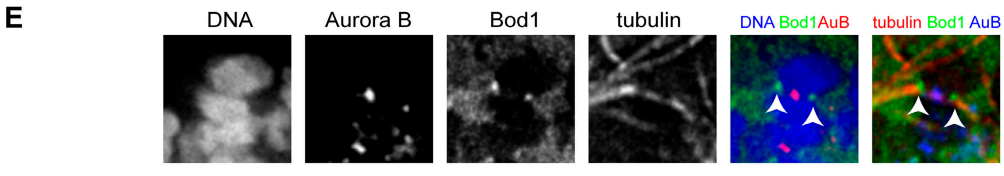

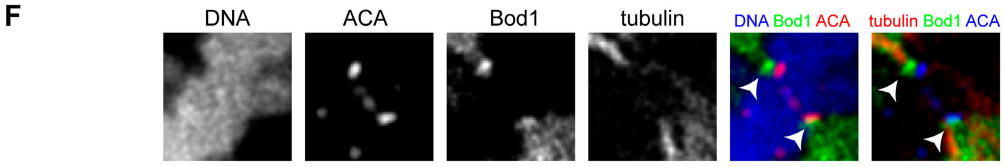

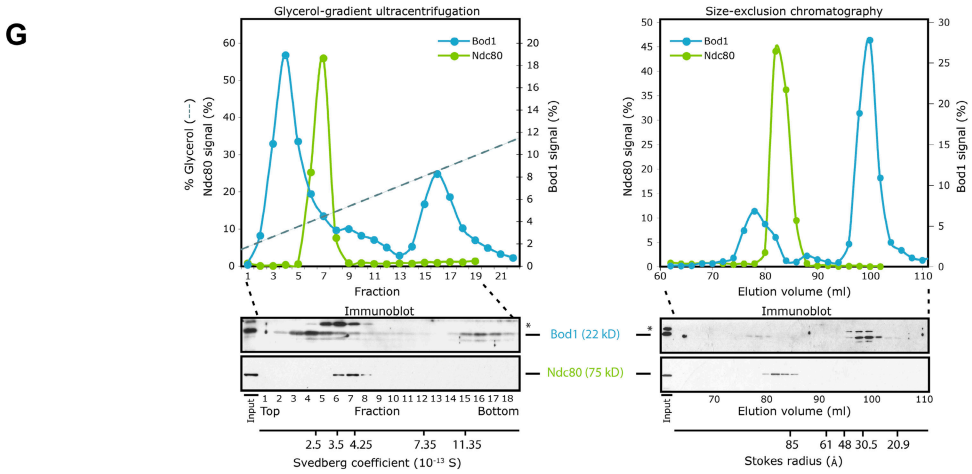

Analysed Protein	Predicted molecular mass (kD)	Subcomplex	Svedberg coefficient (10^{-13} s)	Stokes radius (Å)	Native molecular mass (kD)	f/fo
Bod1	19.3	BOD1 complex (1)	1.78 ± 0.7	34.38 ± 2.6	25.2 ± 10	1.7 ± 0.7
		BOD1 complex (2)	9.97 ± 0.8	118.90 ± 15.6	489.6 ± 76	2.1 ± 0.4
Ndc80	75	NDC80 complex	4.9 ± 0.7	88.6 ± 5.9	177.3 ± 26	2.45 ± 0.4

Figure 1. **Bod1 is a novel protein localizing to centrosomes and kinetochores.** (A and B) Selected maximum intensity projections from time-lapse images of HeLa cells show gene-specific mitotic phenotypes. Cells were transfected with the pU6YH plasmid expressing scrambled shRNA (A) or shRNA targeting Bod1 (B). Images were taken 60 h after transfection over a period of 60–120 min. Numbers indicate time (minutes) from the establishment of a metaphase plate. (C) HeLa cells transfected with Bod1-GFP were fixed after 48 h with PFA. (top) Localization of Bod1-GFP at various points in the cell cycle. (bottom) A merged image with microtubules (red), chromosomes (blue), and Bod1-GFP (green). Arrowheads indicate concentrations of Bod1-GFP at microtubule ends. Insets are magnified images of boxed areas. (D) Chromosome spreads of nocodazole-arrested HeLa cells stained for endogenous Bod1 (green), ACA (red), and DNA (blue).

We have subsequently used liquid chromatography tandem mass spectrometry to characterize our preparations of solubilized *Xenopus* mitotic chromosome proteins. In this study, we have selected four of the unknown chromosome proteins identified in this primary proteomics screen for further characterization. We have investigated the function of their human homologues using a secondary screen based on time-lapse fluorescence imaging of mitotic progression after RNAi-mediated depletion of each unknown. This analysis has identified Bod1, a novel vertebrate centrosomal and outer kinetochore protein that is required for proper chromosome biorientation.

Results and discussion

RNAi phenotypic analysis of unknown proteins

Mass spectrometric analysis identified >250 proteins that associate with chromosomes assembled in metaphase *Xenopus* egg extracts. Experimental details and results of the chromatin proteomic data are deposited at http://www.ebi.ac.uk/pride (*Xenopus* chromatin proteome survey). We chose four of these proteins that were novel, uncharacterized, and had well-conserved orthologues in other species (FLJ13263, ABCF, NPL4, and FAM44B; Fig. S1 B, available at http://www.jcb.org/cgi/content/full/jcb.200704098/DC1). To determine whether these proteins were involved in the generation of condensed chromosomes or in chromosome segregation, we constructed the pU6YH vector that expresses histone H2B-YFP (Platani et al., 2002) and a short hairpin RNA (shRNA) against the target protein (Fig. S1, A and C). The expression of histone H2B-YFP allows the visualization of chromosomes and simultaneously marks cells that are transfected with the shRNA-containing vector. In control experiments with pU6YH coding for shRNA targeting Aurora B, cells expressing histone H2B-YFP always showed knockdown of the target protein, but the amount of histone H2B-YFP detected was poorly correlated with the level of Aurora B knockdown (unpublished data). Regardless, the knockdown was efficient enough to allow us to screen for mitotic phenotypes by monitoring chromosome dynamics by time-lapse imaging of living cells.

Figs. 1 (A and B) and S1 (D–G) show maximum intensity projections of selected time points from time-lapse videos for each targeted protein. Cells expressing shRNA to FLJ3263 or ABCF generally proceeded through mitosis with no obvious phenotypes, similar to control cells expressing scrambled shRNA (Fig. 1 A) or shRNA targeting paraspeckle component 1 (PSP1; Fig. S1 D), a nuclear protein that shows no mitotic phenotype upon depletion by siRNA (Fox et al., 2002). In contrast, cells expressing shRNA targeting Npl4 or Fam44B showed marked mitotic defects. Cells depleted of Npl4 either failed to form a defined metaphase plate (Fig. S1 G) or persisted in metaphase to the end of the experiment (not depicted). Upon entry into anaphase, we often observed the apparent formation of multipolar spindles resulting in cut phenotypes. Cells depleted of Fam44B generally failed to form an organized metaphase plate and maintained this state for extended periods of time before entering an aberrant anaphase with a classic cut phenotype (Fig. 1 B).

The frequency of aberrant anaphase events is quantified in Fig. S1 H. Transfection of plasmids bearing cassettes coding for scrambled shRNA or shRNAs targeting PSPC1, FLJ13263, or ABCF1 caused a low level of aberrant anaphases, whereas the depletion of Npl4 or Fam44B resulted in anaphase defects in 75–80% of cell divisions. After this work was completed, a paper was published describing the function of Npl4 in the regulation of mitotic spindle assembly (Cao et al., 2003). This gave us confidence that our screens are identifying proteins with important roles in chromosome segregation. The defects observed upon Fam44B depletion strongly suggested that this novel protein is required for proper function of the mitotic spindle and possibly for the interactions between kinetochores and microtubules. Because our further characterization showed that Fam44B (provisionally named as a member of a protein family of unknown function) is required for chromosome biorientation, we have named this protein Biorientation Defective 1 (Bod1).

Bod1 is present at human kinetochores

To characterize endogenous Bod1, we generated a Bod1 polyclonal antibody using a recombinant protein antigen. This antibody recognized a 22-kD protein on immunoblots of HeLa cell lysates (Fig. S2 A, available at http://www.jcb.org/cgi/content/full/jcb.200704098/DC1), Bod1-GFP in human cells (Fig. S2 A), and recombinant Bod1 expressed in *Escherichia coli* (not depicted). We were unable to detect Bod1 in HeLa cells by standard immunofluorescence protocols but did detect Bod1 at kinetochores of nocodazole-arrested cells subjected to swelling and spreading using an antibody raised against recombinant Bod1 (Fig. 1 D). This suggests that Bod1 is a component of mitotic kinetochores.

To more fully characterize the properties of Bod1 through the cell cycle, we constructed a Bod1-GFP fusion and used fluorescence microscopy to localize Bod1-GFP. Fig. 1 C shows representative fixed cell images of Bod1-GFP throughout interphase and mitosis 48 h after transfection. Bod1-GFP localized strongly to centrosomes throughout the cell cycle, only dissociating during cytokinesis (Fig. 1 C). Bod1-GFP also localized at kinetochores from prometaphase until anaphase (Fig. 1 C, arrowheads). During metaphase and anaphase, levels of centrosome-bound Bod1 decreased, whereas levels increased on spindle microtubules. To further refine the kinetochore localization of Bod1, we compared the localization of Bod1-GFP with Aurora B (to mark the inner centromere) or anticentromere antibody (ACA; to mark the inner kinetochore; Fig. 1, E and F). The localization of Bod1-GFP was separate from Aurora B and adjacent to, but not overlapping, ACA, suggesting that Bod1 is a component of the outer kinetochore.

(E and F) The localization of Bod1-GFP was determined with respect to Aurora B (E) and ACA (F). Kinetochore localization of Bod1-GFP is indicated by arrowheads. (G) Hydrodynamic analysis of nocodazole-arrested HeLa lysates by glycerol gradient centrifugation (left) and size exclusion chromatography (right) showing that Bod1 is present in two different complexes. Asterisks mark cross-reacting bands. Bars, (A and B), 10 μm; (C), 5 μm.

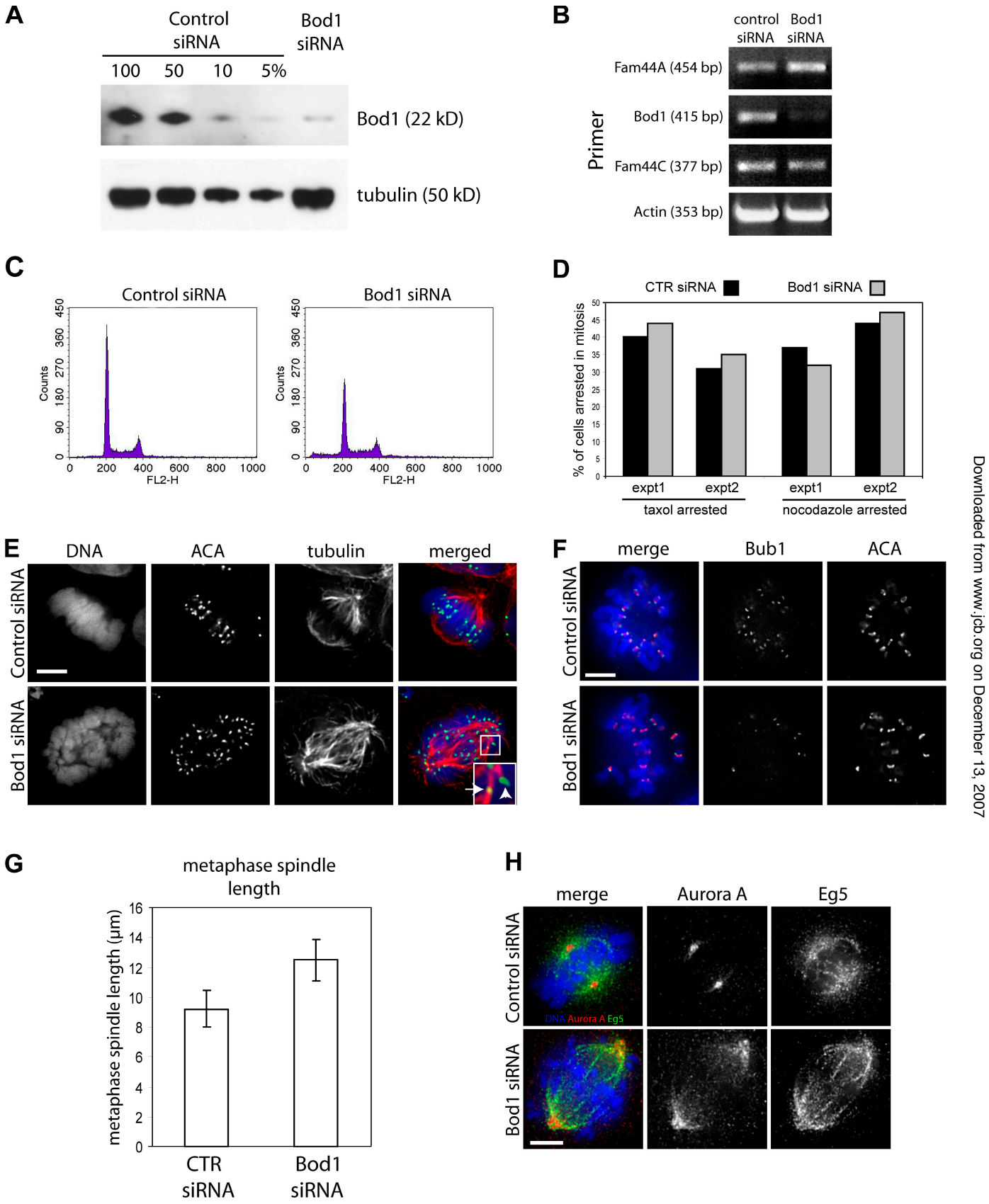

Figure 2. **Depletion of Bod1 by siRNA causes major chromosome alignment defects.** (A) Immunoblot using an anti-Bod1 antibody showing the effective depletion of Bod1 72 h after transfection of siRNA duplexes. Tubulin was used as a loading control. (B) One-step RT-PCR analysis of control and Bod1 siRNA RNA lysates showing the specific knockdown of Bod1 in relation to other Fam44 family members. (C) FACS analysis of control and Bod1-depleted cells. (D) Taxol or nocodazole was added to control or Bod1 siRNA cells 48 h after transfection, and the percentage of mitotic cells was determined

By comparing the fluorescence detected from cells expressing varying amounts of Bod1-GFP with immunoblots of cell lysates, we determined that endogenous Bod1 is expressed at an ~10× lower amount than the lowest detectable level of Bod1-GFP (Fig. S2 A). This explains why we only detected endogenous Bod1 on chromosome spreads. Nonetheless, the overexpression of Bod1-GFP might cause mislocalization and mitotic defects. We observed no detectable changes in cell cycle progression in cells expressing Bod1-GFP (Fig. S2 B) and no changes in Bod1-GFP localization in cells expressing different amounts of Bod1-GFP (Fig. S2 C), suggesting that the expression experiments are not causing substantial defects in cells progressing through mitosis.

Bod1 is a novel type of vertebrate kinetochore component

The kinetochore of *Saccharomyces cerevisiae* is well characterized; upwards of 70 proteins have been identified as components of separable subcomplexes (De Wulf et al., 2003; McAinsh et al., 2003; Westermann et al., 2003). Therefore, we looked for potential orthologues of Bod1 in *S. cerevisiae*. BLAST searches of the *S. cerevisiae* genome using the entire Bod1 sequence failed to find any matches. Splitting the Bod1 sequence into 4–10 amino acid segments and using the patmatch function (http://www.yeastgenome.org) also failed to find any direct orthologues. However, Bod1 is highly conserved throughout metazoans (Fig. S3 A, available at http://www.jcb.org/cgi/content/full/jcb.200704098/DC1), with clear orthologues in mouse, rat, *Xenopus*, *Drosophila*, and *Anopheles gambiae*. No apparent orthologue could be found in *Caenorhabditis elegans*.

Bod1 is one of three related proteins that comprise the Fam44 protein family in the human genome. These proteins are encoded by genes on three different chromosomal loci (4p16.1, 5q35.2, and 18q21.31 for Fam44A, Bod1, and Fam44C, respectively), suggesting that the three genes have arisen from a gene duplication event. Fig. S3 B demonstrates that Bod1 and Fam44C are most closely related. The N terminus of Fam44A is very similar to Bod1 except that it contains a long string of proline residues at the extreme N terminus. Fam44A is approximately twice as large as the other family members with a large C-terminal extension, which does not appear to relate to any other known protein. Fam44A is conserved among vertebrates, but, given the similarity of Fam44C to Bod1, it is was difficult to distinguish whether there were Fam44C-specific genes in species other than *Pan troglodytes* (GenBank/EMBL/DDBJ accession no. XP_001137664).

To determine whether Bod1 is associated with any other proteins, we examined its hydrodynamic properties. Lysates of nocodazole-arrested HeLa cells were fractionated by gel filtration and sedimentation through glycerol gradients and were analyzed with a polyclonal antibody that recognizes Bod1. Both analyses showed that Bod1 exists in two forms: one that is most likely a monomeric, unbound form and one in a complex of ~490 kD (Fig. 1 G). To date, we have not identified the components of this larger complex but note that Ndc80/Hec1, a fundamental component of the kinetochore (DeLuca et al., 2005), does not comigrate with this complex. Further characterization will be necessary to determine whether the large Bod1 complex is a component of the kinetochore or a spindle pole–associated complex.

Bod1 depletion causes major chromosome biorientation defects

Bod1 was depleted from HeLa cells by targeting three different sequences by siRNA (see Materials and methods), resulting in efficient depletion of the protein (Fig. 2 A and not depicted). This depletion was specific, as we observed no change in the levels of Fam44A or Fam44C by RT-PCR (Fig. 2 B).

FACS analysis showed that Bod1^{siRNA} treatment reduced the proportion of G1 cells and caused a substantial increase in apoptotic cells with a sub-G1 DNA content (Fig. 2 C). This increase in the apoptotic population was also confirmed by counting the number of apoptotic cells in fixed DAPI-stained samples. Only 0.47 ± 0.01% of control cells were apoptotic compared with 3.9 ± 0.4% of Bod1^{siRNA}cells.

To assess any effects on the mitotic spindle checkpoint, we treated Bod1^{siRNA} HeLa cells with either nocodazole or taxol and counted phospho-H3–positive cells. In both cases, we observed a robust mitotic arrest, suggesting that the depletion of Bod1 does not impair the spindle checkpoint (Fig. 2 D). In addition, immunostaining Bod1^{siRNA} cells with anti-Bub1 (Fig. 2 F), anti-BubR1, or anti-Mad2 antisera (not depicted) demonstrated that the majority of unaligned kinetochores stained strongly for spindle assembly checkpoint proteins.

Detailed examination of Bod1^{siRNA} HeLa cells by immunofluorescence revealed the presence of somewhat elongated disorganized bipolar mitotic spindles with a mean pole–pole distance of 12.5 μm compared with 9.2 μm in control cells (Fig. 2 G). Given the disorganization of the mitotic spindle, we examined the localization of Eg5 and Aurora A (Fig. 2 H). Although Eg5 localized properly to spindles, which is consistent with the formation of a bipolar spindle, Aurora A staining was much less focused in Bod1^{siRNA} cells, suggesting that Bod1 may play a role in organization of the spindle pole.

Bod1^{siRNA} cells contained many unaligned chromosomes (Fig. 2, E–G). All kinetochores of unaligned chromosomes formed either end-on or lateral attachments with spindle microtubules (Fig. 2 E, inset), with frequent syntelic microtubule–kinetochore attachments (Fig. 3). In addition, all unaligned chromosomes still had robust Hec1 and Mis12 staining at kinetochores, suggesting that after the depletion of Bod1, at least two critical kinetochore subcomplexes were still targeted properly (unpublished data).

18 h later. (E) HeLa cells were transfected with control siRNA or siRNA against Bod1 and processed for immunofluorescence 72 h later. Microtubules are shown in red, chromosomes are shown in blue, and ACA is shown in green. The inset is a magnified image of the boxed area. The arrow shows lateral attachment, and the arrowhead shows end-on attachment. (F) Control or Bod1 siRNA–transfected HeLa cells stained with Bub1 and ACA. (G) The spindle length of control cells and Bod1 siRNA cells. Error bars show SD. (H) Anti-Eg5 and anti–Aurora A staining of control and Bod1 siRNA–transfected HeLa cells. Bars, 5 μm.

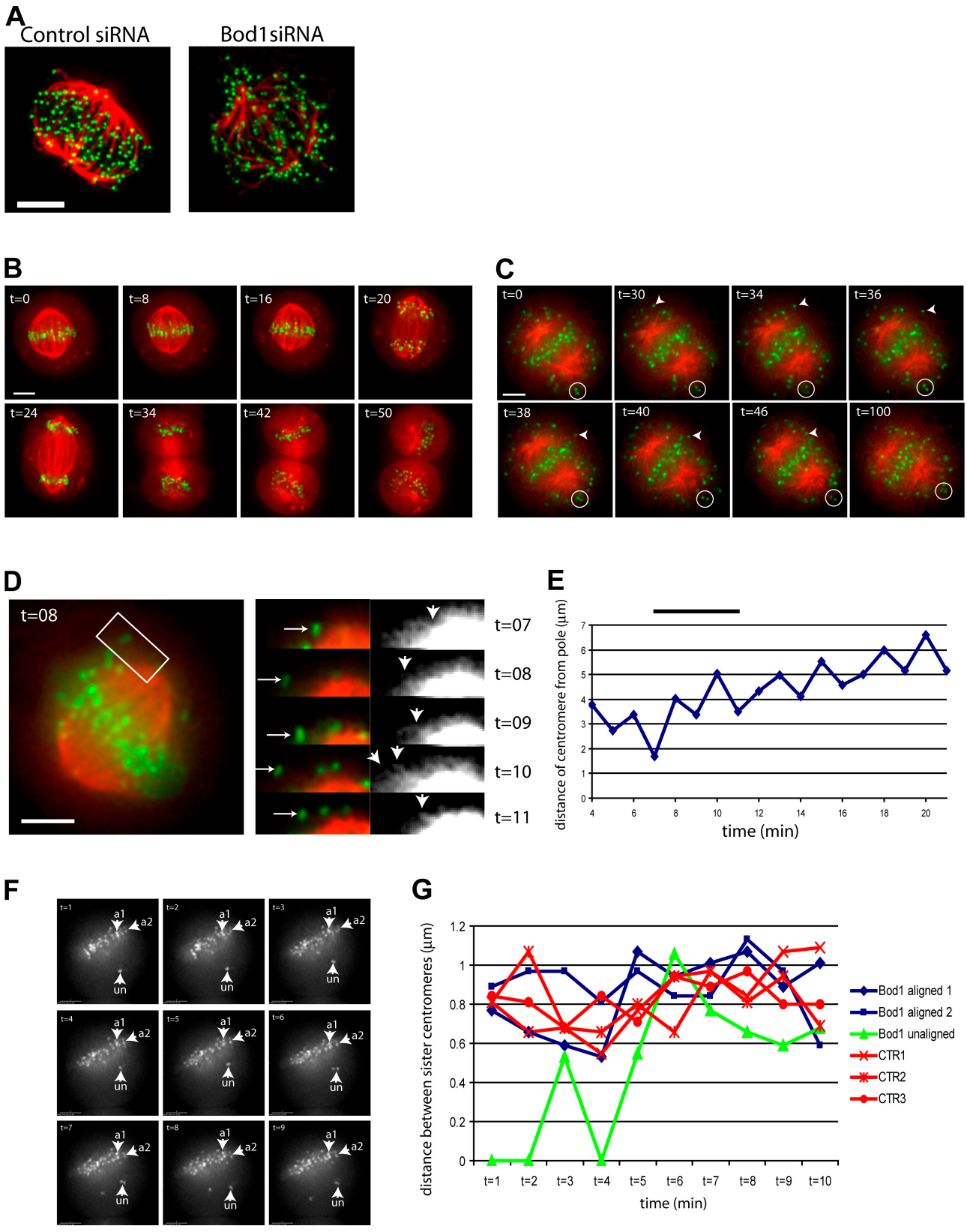

Figure 3. **Microtubule and kinetochore dynamics in Bod1-depleted cells.** (A) Cold stable microtubule assay of control and Bod1-depleted cells. Microtubules are shown in red, and ACA is shown in green. (B–D) Cells were imaged by transiently transfecting either control or Bod1 siRNA, mCherry-tubulin (red), and GFP–CENP-B (green). Imaging was started 72 h after transfection. (B) Projections of selected time points from a cell transfected with control siRNA are shown. Time from the onset of imaging is shown in the top left corner. (C) Cells transfected with Bod1 siRNA failed to align many of their chromosomes. Arrowheads highlight unaligned kinetochores becoming bioriented. Circles highlight pairs of sister kinetochores that remain behind the spindle pole. (D) Bod1-depleted cell showing unaligned sister kinetochores (boxed area). (right) Oscillation of sister kinetochores over 4 min. Black and white panels

These results suggest that after Bod1 depletion, kinetochores can form end-on and lateral attachments to microtubules but, in many cases, cannot achieve correct alignment on the metaphase plate.

Force and oscillations at syntelic attachments in Bod1^{siRNA} cells

Unaligned kinetochores in Bod1^{siRNA} cells might be unable to congress to the metaphase plate because of defects in microtubule attachments or microtubule plus end dynamics. Alternatively, the microtubule attachments might be functional, but syntelic attachments might be inappropriately stabilized. To discern between these possibilities, we performed a cold stable kinetochore fiber assay. Fig. 3 A shows that although the overall density of microtubules was reduced, all kinetochores in Bod1^{siRNA} cells were attached to microtubules after cold treatment, as in control cells. To assess the function of these attachments, we cotransfected Bod1^{siRNA} cells with plasmids expressing GFP–centromere protein B (CENP-B) and mCherry-tubulin (see Materials and methods). Fig. 3 (B and C) shows stills from time-lapse videos of projections of control and Bod1^{siRNA} cells. Control cells formed normal mitotic spindles, achieved normal chromosome alignment, and progressed through mitosis (Fig. 3 B and Video 1, available at http://www.jcb.org/cgi/content/full/jcb.200704098/DC1). In contrast, Bod1^{siRNA} cells aligned some chromosomes but contained many misaligned chromosomes (Fig. 3 C and Videos 2–4). The severity of this phenotype varied, with some cells showing a small number of misaligned chromosomes and others showing many chromosomes on the distal side of spindle poles (Video 2). Most misaligned chromosomes were associated with end-on attachments to microtubule bundles and underwent oscillatory movements (Fig. 3, D and E; and Videos 3 and 4).

Sister centromeres normally only separate when under tension in a bioriented state (Waters et al., 1996). In Bod1^{siRNA} cells expressing GFP–CENP-B and mCherry-tubulin, we observed the oscillatory separation of unaligned sister centromeres. These centromeres appeared to be syntelically attached to a bundle of microtubules, and sister centromere separation was not aligned with the pole–pole axis (Fig. 3 F, "un" arrowhead; and Video 4). This observation was confirmed by time-lapse analysis by measuring distances between two bioriented sister centromeres (used as an internal control) and an unaligned pair of sister centromeres in a Bod1^{siRNA} cell (Fig. 3, F and G). We conclude that kinetochores on misaligned sister chromosomes were attached syntelically to microtubules from the neighboring pole and that the separation of misaligned sister centromeres reflects asynchronous microtubule end dynamics on a centromere pair, resulting in force across the pair. Kinetochores in Bod1^{siRNA} cells can therefore attach to microtubule ends and generate force, and the major defect in Bod1^{siRNA} cells appears to be an inability to detect or resolve syntelic microtubule attachments.

Syntelic attachments persist in Bod1-depleted cells

The mitotic profile of Bod1^{siRNA} cells was very similar to control cells except for a marked increase in cells with major biorientation defects and a corresponding decrease in normal metaphase cells (Fig. 4 A). Given the severity of the biorientation defect, we were surprised not to see an increase in aberrant anaphases. Long-term time-lapse imaging of cells cotransfected with CENP-B–GFP and control or Bod1 siRNA (Fig. 4 B) revealed that the biorientation defect in Bod1^{siRNA} cells would persist for up to 12 h before cells either directly entered apoptosis or exited mitosis and apoptosis several hours later, explaining why a high rate of aberrant anaphases were not observed.

To determine whether the biorientation defects in Bod1^{siRNA} cells were caused by a failure to resolve syntelic attachments, we artificially increased the occurrence of these attachments by the addition of the drug monastrol, which causes monopolar spindles and results in the majority of kinetochore microtubule attachments being syntelic (Kapoor et al., 2000). Fig. 4 C shows that Bod1^{siRNA} cells arrest as efficiently as control cells with monopolar spindles when treated with monastrol. 1 h after release from monastrol into media containing MG132, to prevent cells going into anaphase, 60% of control cells formed a fully aligned metaphase plate with virtually no biorientation defects. In contrast, only 37% of mitotic Bod1^{siRNA} cells had properly aligned their chromosomes, and 26% had severe biorientation defects. Detailed inspection by immunofluorescence demonstrated that these cells contained syntelic attachments (Fig. 4 D). Therefore, by artificially increasing the number of syntelic attachments in Bod1-depleted cells, we increased the frequency of biorientation defects from 15% in unperturbed cells to 26% in cells released from the monastrol block (Fig. 4, A and C). We conclude that the depletion of Bod1 compromises the efficient resolution of syntelic attachments.

Phosphorylation of MCAK is reduced in Bod1^{siRNA} cells

The destabilization of syntelic attachments allowing subsequent correction requires the Aurora B protein kinase (Ditchfield et al., 2003; Hauf et al., 2003). Aurora B phosphorylates mitotic centromere-associated kinesin (MCAK; and possibly Kif2), and this phosphorylation appears to be required for this destabilization (Andrews et al., 2004; Lan et al., 2004; Ohi et al., 2004). Therefore, we analyzed the localization and phosphorylation of MCAK in Bod1-depleted cells. After Bod1 depletion, Aurora B still localized to mitotic chromosomes, and we detected no

show saturated images of tubulin staining to highlight microtubules. Arrows show single oscillating kinetochore pairs; arrowheads show oscillating microtubules. (E) The distance between the sister kinetochores highlighted in D and the centrosome were plotted over time. The black bar highlights the measurements taken from images in D. (F) Selected time points from a Bod1-depleted cell showing CENP-B–GFP. (G) The distance between kinetochores in the unaligned sisters (green line; "un" arrowheads in F) and aligned sisters (aligned 1 and aligned 2, blue lines; a1 and a2 arrowheads in F) depicted in F were measured over time. The distance between three selected sister kinetochore pairs from control cells were also measured over time (red lines). Bars, 10 μm.

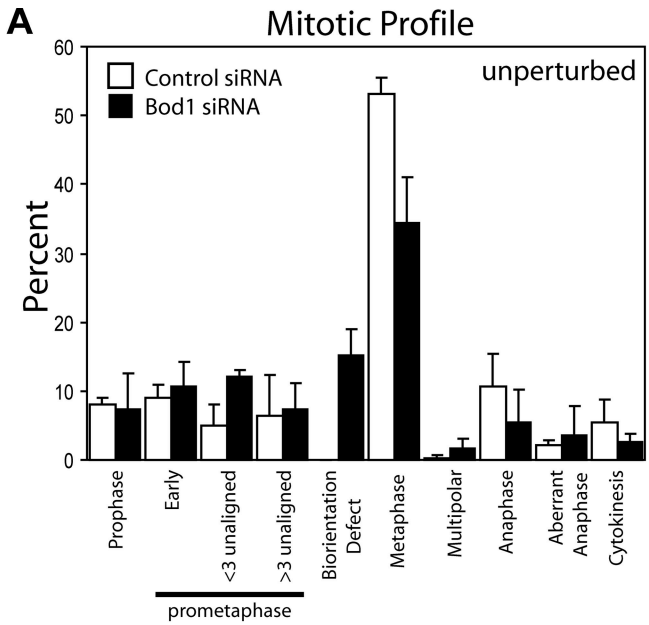

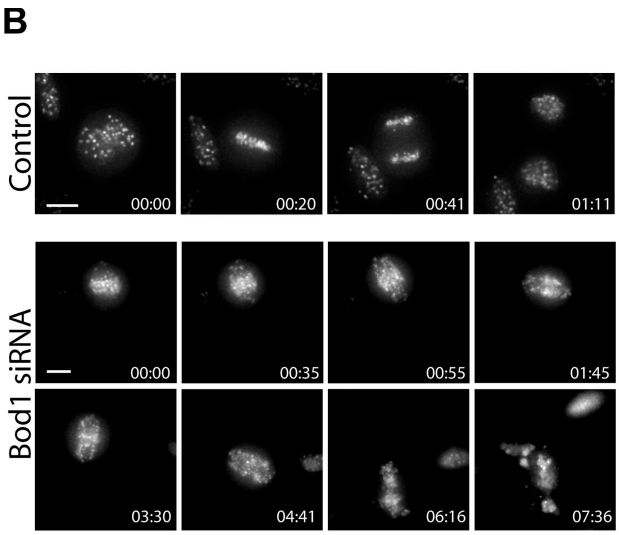

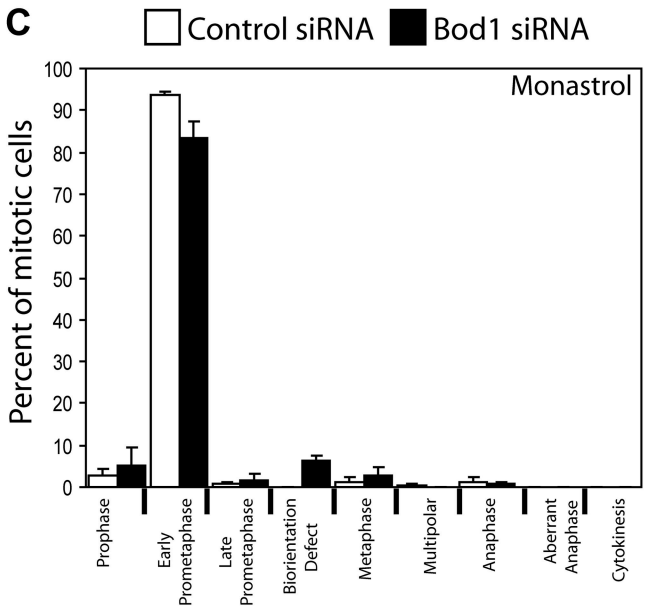

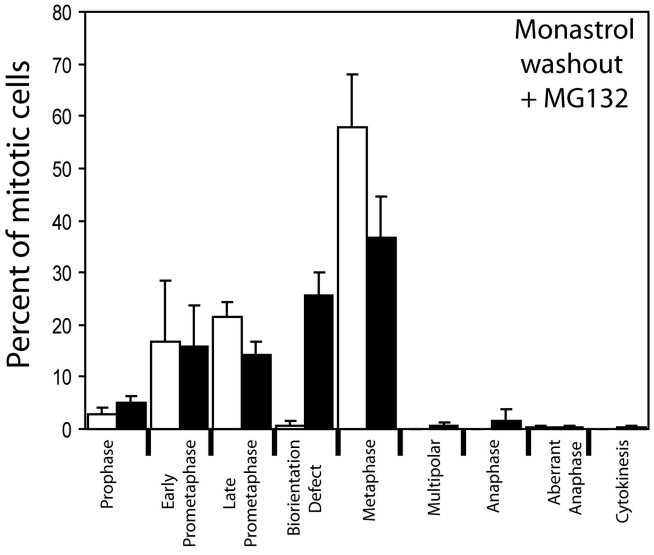

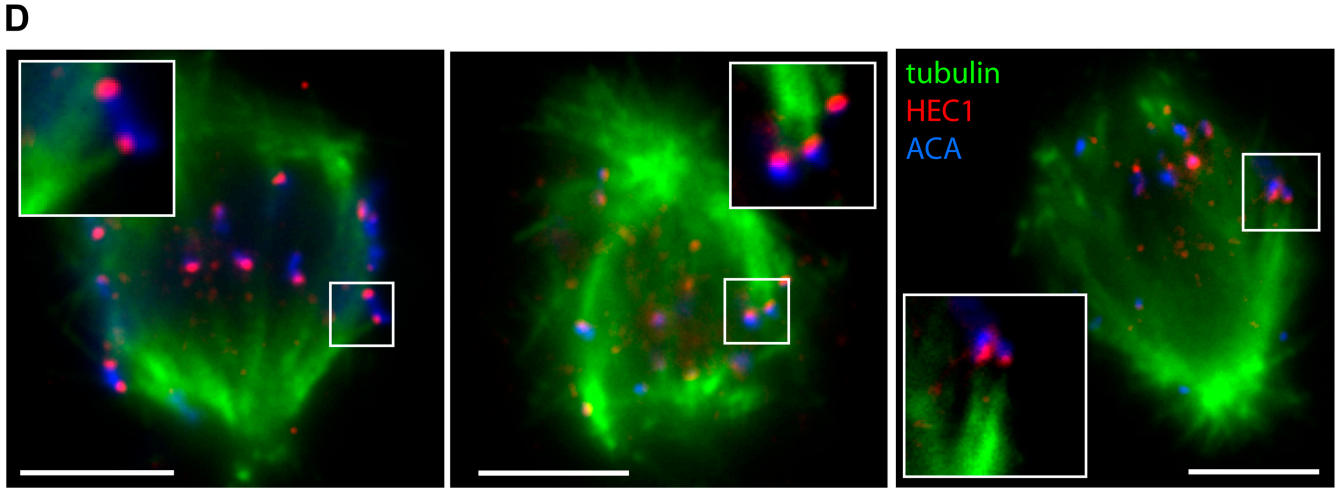

difference in the amount of Aurora B in unaligned and apparently aligned chromosomes (Fig. 5 A). We detected no change in chromosome staining with anti–phosphohistone H3 (Fig. 5 A) or anti-phospho–CENP-A (not depicted) after Bod1 depletion. Because both are markers of Aurora B activity (Zeitlin et al., 2001), these results suggest that Aurora B kinase activity was not dramatically impaired by the loss of Bod1. To further assay the function of Aurora B, we determined the localization of MCAK, which localizes to the inner centromere in its phosphorylated form but concentrates at kinetochores in its dephosphorylated state (Andrews et al., 2004). At unaligned sister kinetochores or in kinetochore pairs not yet fully under tension, MCAK is predominantly located at the inner centromere (Fig. 5 B; Andrews et al., 2004). In Bod1^{siRNA} cells, we observed that although total MCAK present at unaligned centromeres was similar to control cells (Fig. 5 C), its precise localization was abnormal, forming multiple foci stretching out to one or both sister kinetochores.

Because MCAK localization to centromeres and kinetochores depends on the state of MCAK phosphorylation, we examined the levels of phosphorylated MCAK using an anti–phospho-Ser92 MCAK antibody (Andrews et al., 2004). Phosphorylation of MCAK was substantially reduced at the inner centromere of unaligned chromosomes in Bod1^{siRNA} cells compared with the control cells (Fig. 5, D and E). These results suggest that Bod1 depletion impairs the formation of bioriented attachments across sister kinetochores, possibly by impairing the correct localization of MCAK at centromeres and, thereby, preventing its phosphorylation and timely correction of syntelic attachments. We have not detected any effect of Bod1 on the in vitro phosphorylation of MCAK by Aurora B (unpublished data), so Bod1 may modulate MCAK phosphorylation by interacting with other proteins. Aurora B activity and kinetochore oscillations are necessary for syntelic correction (Lampson et al., 2004), and our data further suggest that syntelic correction may require MCAK phosphorylation. Whether there is any subtle perturbation in kinetochore oscillations in Bod1-depleted cells is not yet known and will require much higher resolution live cell imaging.

In summary, by using a cell cycle–dependent analysis of the *Xenopus* chromatin proteome, we have identified a novel protein required for proper chromosome biorientation called Bod1. Bod1 is a member of the FAM44 protein family and is highly conserved throughout metazoans. Depletion of Bod1 in human cells causes severe biorientation defects, although kinetochores appear to generate force and oscillate. Bod1 is not required for the spindle assembly checkpoint but appears to be required either for the efficient detection or removal of syntelic attachments. Thus, it plays a critical role in defining and monitoring the proper attachment of microtubules to the kinetochore.

Materials and methods

Tissue culture

HeLa S3 cells were grown in DME supplemented with 10% FCS, 2 mM L-glutamine, 100 U/ml penicillin, and 100 μg/ml streptomycin (Invitrogen) at 37°C with 5% CO_2 in a humidified incubator.

shRNA depletion of target proteins and time-lapse imaging

HeLa cells were transfected with pU6YH plasmid (Fig. S1) encoding shRNAi to Bod1 or other target proteins. 48 h after transfection, cells were split onto 40-mm-diameter glass coverslips (Bioptechs), cultured overnight, and transferred to CO_2 independent media (Invitrogen) with supplements as above. Cells were maintained at 37°C using an FCS2 chamber in conjunction with an objective heater (Bioptechs). Images were acquired on a restoration microscope (DeltaVision Spectris; Applied Precision) with a 100× 1.35 NA objective and a cooled charge-coupled device camera (CoolSNAP HQ; Roper Scientific). SoftWorx software (Applied Precision) was used for image analysis. Datasets were deconvolved using the constrained iterative algorithm (Swedlow et al., 1997; Wallace et al., 2001) using SoftWorx software. Time courses were presented as maximum intensity projections of deconvolved three-dimentional datasets. Images were loaded into Photoshop (Adobe) or OMERO (http://openmicroscopy.org) and adjusted for display.

siRNA depletion of Bod1

To deplete Bod1, HeLa cells were transfected with siRNA duplexes targeting the sequence UUCAUGAGUUCCUGGCGGCTT (MWG Biotech) or STEALTH siRNA duplexes (Invitrogen) targeting the sequences GCCACAAAUAGAACGAGCAAUUCAU or GGAAUGGAAUCCUACGAUGAACAAA for 48 or 72 h. Scrambled siRNA duplexes were used as controls. RT-PCR analysis was performed using a One Step RT-PCR kit (QIAGEN) according to the manufacturer's instructions.

Time-lapse imaging of mCherry-tubulin and CENP-B–GFP in siRNA-treated HeLa cells

HeLa cells were cotransfected with mCherry1 (Shaner et al., 2004) fused to human β-tubulin (a gift from A. Straight, Stanford University, Stanford, CA), CENP-B–GFP (a gift from V. Draviam and P. Sorger, Harvard Medical School, Boston, MA), and either control or Bod1 siRNA. 24 h after transfection, cells were trypsinized and seeded onto 35-mm glass-bottom Microwell dishes (MatTek Corp.). Imaging was started 48 or 72 h after transfection. Datasets (512 × 512 pixels with 2 × 2 binning, 0.05-s exposure, and five z sections spaced by 0.5 μm) were acquired every 1 or 2 min on a microscope (DeltaVision Spectris; Applied Precision) fitted with a 37°C environmental chamber (Solent).

Bod1 antibody generation

Anti–human Bod1 antibody was generated against recombinant GST-Bod1 fusion and used to immunize rabbits (Diagnostics Scotland). The antibody was affinity purified by incubating serum with recombinant myelin basic protein–Bod1 conjugated to Affigel 10 active ester agarose (Bio-Rad Laboratories).

Hydrodynamic analysis

Mitotic cell extracts were prepared from HeLa cells treated with 100 ng/ml nocodazole for 16 h. Size exclusion chromatography and glycerol density gradients were performed as previously described (De Wulf et al., 2003) except that 5-ml gradients and H150 buffer (50 mM Hepes, 150 mM KCl, 1 mM EDTA, and 1 mM $MgCl_2$, pH 7.9) were used. The native molecular weight and shape (frictional coefficient) of protein complexes was calculated using established equations (Siegel and Monty, 1965; Harding and Colfen, 1995; Schuyler and Pellman, 2002).

Immunofluorescence

Cells were fixed with 3.7% PFA or in methanol for 2 min at −20°C and processed as described previously Andrews et al. (2004). Aqueous chromosome spreads were performed as described previously (Earnshaw et al., 1989).

Figure 4. **Bod1 is required for the efficient resolution of syntelic attachments.** (A) The mitotic profile of control and Bod1-depleted cells was determined 72 h after transfection of siRNA. (B) GFP–CENP-B–transfected HeLa cells were cotransfected with control or Bod1 siRNA, and time-lapse microscopy was performed 72 h after transfection. Projections of selected time points are shown. (C) Control or Bod1 siRNA HeLa cells were treated with monastrol for 3 h, washed, and released into media containing MG132 for 1 h before fixing. The mitotic profile before and after monastrol release is shown. (D) Syntelic attachments in Bod1 siRNA cells 1 h after release from monastrol showing microtubules (green), anti-Hec1 (red), and ACA (blue). Insets are magnified images of boxed areas. Error bars represent SD. Bars, 5 μm.

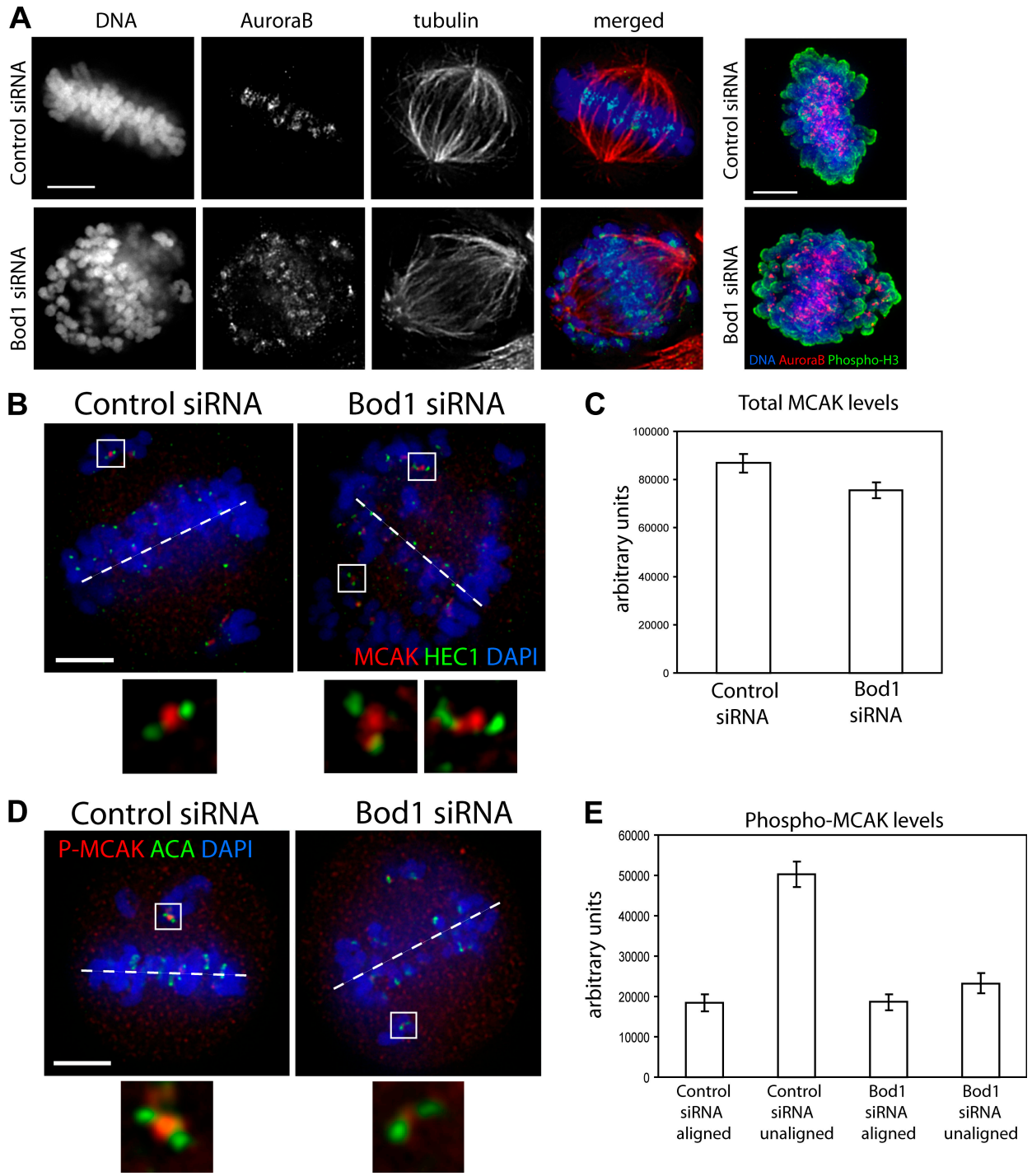

Figure 5. **MCAK is not efficiently phosphorylated in Bod1^{siRNA} cells.** (A) Aurora B is not delocalized in Bod1-depleted cells. Phospho-Ser10-histone H3 staining in control and Bod1 siRNA cells indicating Aurora B activity. (B–E) Cells were transfected with control or Bod1 siRNA. After 72 h, cells were treated with monastrol for 3 h and released into media containing MG132 for 1 h before fixing. (B and C) Cells were stained for total MCAK population, and levels at kinetochores were quantified. Boxed areas are magnified below the main images. (D and E) Cells were stained for phospho-Ser92-MCAK, and levels at aligned and unaligned kinetochores were quantified. Dashed lines indicate orientation of the metaphase plate. Error bars represent SD. Bars, 5 μm.

Mouse anti–α-tubulin DM1A (Sigma-Aldrich), rabbit anti-HEC1 antibody (Abcam), mouse anti–Aurora B antibody AIM-1 (BD Biosciences), and mouse anti-Bub1 (Chemicon) were used at 1:500. Rabbit anti–Aurora A (Abcam), mouse anti-Eg5 (BD Biosciences), and human CREST autoantisera (ACA; a gift from W.C. Earnshaw, University of Edinburgh, Edinburgh, Scotland, UK) were used at 1:1,000. Sheep anti-MCAK and anti–phospho-MCAK antibodies (Andrews et al., 2004) were used at 1 μg/ml. Rabbit anti–phospho-H3 (Ser10; Upstate Biotechnology) was used at 1:200. Fluorescently labeled secondary antibodies were all obtained from Jackson ImmunoResearch Laboratories.

Online supplemental material

Fig. S1 shows the use of shRNAi and live cell imaging to identify candidate proteins. Fig. S2 shows the relative expression levels of Bod1-GFP. Fig. S3

shows Fam44 protein family sequence alignment. Videos 1–4 are videos relating to stills shown in Fig. 3. Online supplemental material is available at http://www.jcb.org/cgi/content/full/jcb.200704098/DC1.

We thank Bill Earnshaw, Aaron Straight, Viji Draviam, Peter Sorger, and Neil Perkins for reagents and members of the Swedlow and Blow laboratories for helpful discussions and criticism.

This work was supported by Cancer Research UK grants C303/A3135 to J.J. Blow and C303/A5434 and C303/A2337 to J.J. Blow and J.R. Swedlow. A.D. McAinsh and S.E. McClelland were supported by Marie Curie Cancer Care. J.R. Swedlow is a Wellcome Trust Senior Research Fellow.

Submitted: 17 April 2007
Accepted: 22 September 2007

References

Andrews, P.D., Y. Ovechkina, N. Morrice, M. Wagenbach, K. Duncan, L. Wordeman, and J.R. Swedlow. 2004. Aurora B regulates MCAK at the mitotic centromere. *Dev. Cell*. 6:253–268.

Cao, K., R. Nakajima, H.H. Meyer, and Y. Zheng. 2003. The AAA-ATPase Cdc48/p97 regulates spindle disassembly at the end of mitosis. *Cell*. 115:355–367.

Cheeseman, I.M., S. Niessen, S. Anderson, F. Hyndman, J.R. Yates III, K. Oegema, and A. Desai. 2004. A conserved protein network controls assembly of the outer kinetochore and its ability to sustain tension. *Genes Dev.* 18:2255–2268.

Cleveland, D.W., Y. Mao, and K.F. Sullivan. 2003. Centromeres and kinetochores: from epigenetics to mitotic checkpoint signaling. *Cell*. 112:407–421.

De Wulf, P., A.D. McAinsh, and P.K. Sorger. 2003. Hierarchical assembly of the budding yeast kinetochore from multiple subcomplexes. *Genes Dev.* 17:2902–2921.

DeLuca, J.G., Y. Dong, P. Hergert, J. Strauss, J.M. Hickey, E.D. Salmon, and B.F. McEwen. 2005. Hec1 and nuf2 are core components of the kinetochore outer plate essential for organizing microtubule attachment sites. *Mol. Biol. Cell*. 16:519–531.

Desai, A., H.W. Deacon, C.E. Walczak, and T.J. Mitchison. 1997. A method that allows the assembly of kinetochore components onto chromosomes condensed in clarified *Xenopus* egg extracts. *Proc. Natl. Acad. Sci. USA*. 94:12378–12383.

Ditchfield, C., V.L. Johnson, A. Tighe, R. Ellston, C. Haworth, T. Johnson, A. Mortlock, N. Keen, and S.S. Taylor. 2003. Aurora B couples chromosome alignment with anaphase by targeting BubR1, Mad2, and Cenp-E to kinetochores. *J. Cell Biol.* 161:267–280.

Earnshaw, W.C., H. Ratrie III, and G. Stetten. 1989. Visualization of centromere proteins CENP-B and CENP-C on a stable dicentric chromosome in cytological spreads. *Chromosoma*. 98:1–12.

Emanuele, M.J., M.L. McCleland, D.L. Satinover, and P.T. Stukenberg. 2005. Measuring the stoichiometry and physical interactions between components elucidates the architecture of the vertebrate kinetochore. *Mol. Biol. Cell*. 16:4882–4892.

Fox, A.H., Y.W. Lam, A.K. Leung, C.E. Lyon, J. Andersen, M. Mann, and A.I. Lamond. 2002. Paraspeckles: a novel nuclear domain. *Curr. Biol.* 12:13–25.

Funabiki, H., and A.W. Murray. 2000. The *Xenopus* chromokinesin Xkid is essential for metaphase chromosome alignment and must be degraded to allow anaphase chromosome movement. *Cell*. 102:411–424.

Harding, S.E., and H. Colfen. 1995. Inversion formulae for ellipsoid of revolution macromolecular shape functions. *Anal. Biochem.* 228:131–142.

Hauf, S., R.W. Cole, S. LaTerra, C. Zimmer, G. Schnapp, R. Walter, A. Heckel, J. Van Meel, C.L. Rieder, and J.M. Peters. 2003. The small molecule Hesperadin reveals a role for Aurora B in correcting kinetochore-microtubule attachment and in maintaining the spindle assembly checkpoint. *J. Cell Biol.* 161:281–294.

Hirano, T., and T.J. Mitchison. 1994. A heterodimeric coiled-coil protein required for mitotic chromosome condensation in vitro. *Cell*. 79:449–458.

Kapoor, T.M., T.U. Mayer, M.L. Coughlin, and T.J. Mitchison. 2000. Probing spindle assembly mechanisms with monastrol, a small molecule inhibitor of the mitotic kinesin, Eg5. *J. Cell Biol.* 150:975–988.

Khoudoli, G.A., I.M. Porter, J.J. Blow, and J.R. Swedlow. 2004. Optimisation of the two-dimensional gel electrophoresis protocol using the Taguchi approach. *Proteome Sci.* 2:6.

Lampson, M.A., K. Renduchitala, A. Khodjakov, and T.M. Kapoor. 2004. Correcting improper chromosome-spindle attachments during cell division. *Nat. Cell Biol*. 6:232–237.

Lan, W., X. Zhang, S.L. Kline-Smith, S.E. Rosasco, G.A. Barrett-Wilt, J. Shabanowitz, D.F. Hunt, C.E. Walczak, and P.T. Stukenberg. 2004. Aurora B phosphorylates centromeric MCAK and regulates its localization and microtubule depolymerization activity. *Curr. Biol.* 14:273–286.

McAinsh, A.D., J.D. Tytell, and P.K. Sorger. 2003. Structure, function, and regulation of budding yeast kinetochores. *Annu. Rev. Cell Dev. Biol.* 19:519–539.

Meraldi, P., A.D. McAinsh, E. Rheinbay, and P.K. Sorger. 2006. Phylogenetic and structural analysis of centromeric DNA and kinetochore proteins. *Genome Biol.* 7:R23.

Murnion, M.E., R.A. Adams, D.M. Callister, C.D. Allis, W.C. Earnshaw, and J.R. Swedlow. 2001. Chromatin-associated protein phosphatase 1 regulates aurora-B and histone H3 phosphorylation. *J. Biol. Chem.* 276:26656–26665.

Ohi, R., T. Sapra, J. Howard, and T.J. Mitchison. 2004. Differentiation of cytoplasmic and meiotic spindle assembly MCAK functions by Aurora B-dependent phosphorylation. *Mol. Biol. Cell*. 15:2895–2906.

Platani, M., I. Goldberg, A.I. Lamond, and J.R. Swedlow. 2002. Cajal body dynamics and association with chromatin are ATP-dependent. *Nat. Cell Biol.* 4:502–508.

Schuyler, S.C., and D. Pellman. 2002. Analysis of the size and shape of protein complexes from yeast. *Methods Enzymol.* 351:150–168.

Shaner, N.C., R.E. Campbell, P.A. Steinbach, B.N. Giepmans, A.E. Palmer, and R.Y. Tsien. 2004. Improved monomeric red, orange and yellow fluorescent proteins derived from *Discosoma* sp. red fluorescent protein. *Nat. Biotechnol.* 22:1567–1572.

Siegel, L.M., and K.J. Monty. 1965. Determination of molecular weights and frictional ratios of macromolecules in impure systems: aggregation of urease. *Biochem. Biophys. Res. Commun.* 19:494–499.

Swedlow, J.R., and T. Hirano. 2003. The making of the mitotic chromosome. Modern insights into classical questions. *Mol. Cell*. 11:557–569.

Swedlow, J.R., J.W. Sedat, and D.A. Agard. 1997. Deconvolution in optical microscopy. *In* Deconvolution of Images and Spectra. P.A. Jansson, editor. Academic Press, San Diego. 284–309.

Tanaka, T.U., M.J. Stark, and K. Tanaka. 2005. Kinetochore capture and bi-orientation on the mitotic spindle. *Nat. Rev. Mol. Cell Biol.* 6:929–942.

Uchiyama, S., S. Kobayashi, H. Takata, T. Ishihara, N. Hori, T. Higashi, K. Hayashihara, T. Sone, D. Higo, T. Nirasawa, et al. 2005. Proteome analysis of human metaphase chromosomes. *J. Biol. Chem.* 280:16994–17004.

Wallace, W., L.H. Schaefer, and J.R. Swedlow. 2001. A workingperson's guide to deconvolution in light microscopy. *Biotechniques*. 31:1076–1097.

Waters, J.C., R.V. Skibbens, and E.D. Salmon. 1996. Oscillating mitotic newt lung cell kinetochores are, on average, under tension and rarely push. *J. Cell Sci.* 109:2823–2831.

Westermann, S., I.M. Cheeseman, S. Anderson, J.R. Yates III, D.G. Drubin, and G. Barnes. 2003. Architecture of the budding yeast kinetochore reveals a conserved molecular core. *J. Cell Biol.* 163:215–222.

Zeitlin, S.G., R.D. Shelby, and K.F. Sullivan. 2001. CENP-A is phosphorylated by Aurora B kinase and plays an unexpected role in completion of cytokinesis. *J. Cell Biol.* 155:1147–1157.